Turkish Journal of Electrical Engineering & Computer Sciences

http://journals.tubitak.gov.tr/elektrik/

Research Article

Turk J Elec Eng & Comp Sci
(2016) 24: 3961 – 3975

doi:10.3906/elk-1412-82

Fuzzy speed estimation in the case of sensorless induction machine vector control

Mohamed BAHLOUL[1,*], Mansour SOUISSI[1], Mohamed CHAABANE[1], Larbi CHRIFI-ALAOUI[2], Said DRID[3]

[1]Laboratory of Sciences and Techniques of Automatic Control and Computer Engineering (Lab-STA), National School of Engineering of Sfax, Sfax, Tunisia

[2]Laboratory of Innovative Technology (LTI), University of Picardie Jules Verne, Cuffies, France

[3]Laboratory of Propulsion Systems (LSPIE), University of Batna, Batna, Algeria

Received: 14.12.2014 • **Accepted/Published Online:** 25.06.2015 • **Final Version:** 20.06.2016

Abstract: This paper deals with the problem of sensorless indirect field oriented control of an induction machine. Based on the fourth-order nonlinear model, we propose a novel structure of a full-order Takagi–Sugeno (TS) adaptive observer, through which we ensure the estimation of IM states and the rotor speed, which is considered as an immeasurable premise variable. This approach satisfies global stability for all operating conditions and operates under unknown applied load torque. In this work, a TS fuzzy model is presented to approximate a nonlinear IM model in the stationary rotating reference frame. A TS adaptive observer is then described. We then design observer gains to guarantee specified observer dynamic performances through a D-stability analysis. Meanwhile, a TS-based scheme is proposed for speed estimation. The synthesis is based on sufficient conditions that are developed and formulated into linear matrix inequalities terms. Simulation and experimental results are given to show the effectiveness of the proposed method.

Key words: Induction machine sensorless control, indirect field oriented control, fuzzy logic, adaptive Luenberger observer, D-stability analysis

1. Introduction

Sensorless field oriented control becomes a major issue in induction machine (IM) control. This research field has been highlighted extensively in the previous few decades due to increasing demand in the industry for a high-performance sensorless control, in order to overcome the drawbacks of sensor implementation within the machine [1]. Unfortunately, the use of sensors increases the weight, the cost, and the electrical sensibility, as well as having an undesirable influence on system reliability. Indeed, much research has focused on the improvement of the sensorless control's performance by using intelligent and sophisticated approaches like the model reference adaptive system observer [2], Kalman filtering [3,4], neural networks [5], the sliding mode observer [6,7], and the Luenberger adaptive observer [8–10].

Over the last few decades, important works have been devoted to using fuzzy logic to cope with the problems of modeling and control of nonlinear systems; interesting results have been proven for its application on IM control [11–13]. Among the fuzzy approaches, the Takagi–Sugeno (TS) method has been widely used, and it has been the subject of many studies [14–16]. Moreover, this method has been associated with many control techniques in order to guarantee some control objectives. We note that the local pole placement of the

*Correspondence: eng.mohamed.bahloul@ieee.org

TS model, based on the D-stability method, has been an attractive research field due to its ability to enhance the system's dynamics performance and robustness [17,18].

Modeling is a critical step in the analysis, diagnostics, or control of the IM. In the literature, many approaches to state space modeling of the IM have been described. However, the nonlinear character remains the common major drawback. One of the innovative solutions for overcoming this problem is the use of the TS approach based on the method of nonlinear sectors [19,20]. This method allows perfect presentation of the IM dynamics in a state space form by means of mathematical convex transformations. In the work of Allouche et al. [21], a TS fuzzy modeling of the IM using the nonlinear sector approach was carried out. Based on the resulting TS IM model, a speed tracking control via fuzzy observer was then discussed. However, the proposed approach remains inadequate for sensorless control due to the observability problem in the model whenever the rotor speed is not measurable. This problem was overcome by Liu et al. [22] and Hung et al. [23], where the authors introduced a TS model for a linear induction machine. Indeed, through a fifth-order nonlinear TS model described by 8 TS local models, the authors successfully solved the problem of sensorless speed control using different methods. However, we may note that the load torque must be known or approximated by a Taylor series based on the primary speed (which limits the use of the proposed results in industrial applications). In addition, the dynamic behavior of the TS observer has not been studied.

Taking into consideration the aforementioned observations, we propose in this paper a sensorless IM vector control approach. Based on a full-order TS adaptive observer, we estimate both the rotor speed and IM states. The TS design is based on a fourth-order TS IM model. Due to the use of this method, the load torque will be considered as an external unknown disturbance. TS observer dynamic performances are thoroughly investigated through a D-stability analysis. The synthesized speed estimation scheme is derived from a stability analysis based on the Lyapunov theory. As a summary, the main contributions of this work could be described in 3 points:

1. An optimal TS IM model is described by means of only 2 TS local models, which is globally observable in the entire speed range.

2. A D-stability of the TS adaptive observer is considered.

3. A novel fuzzy speed estimation scheme for IM sensorless control insensitive to load torque is developed.

The rest of this paper is organized as follows: in Section 2, the IM TS model is described. Section 3 is split into 2 steps. In the first step, we introduce the TS adaptive observer structure. The exponential convergence of estimation errors and the pole placement of the proposed observer are then studied. The proposed results are formulated on the basis of LMI terms (linear matrix inequalities), which can be solved easily using MATLAB tools. In Section 4, an experimental check is carried out to confirm its validity and its performances.

2. TS fuzzy modeling of induction motor

2.1. Dynamic description of induction motor

The induction machine can be presented in the d-q stationary (alpha-beta) reference frame by the following state space model:

$$\begin{cases} \dot{x}(t) = A(t)x(t) + Bu(t) \\ y(t) = Cx(t) \end{cases}, \tag{1}$$

such that:

$$\begin{cases} x(t) = \begin{bmatrix} i_{sd} & i_{sq} & \Psi_{rd} & \Psi_{rq} \end{bmatrix}^T \\ y(t) = \begin{bmatrix} i_{sd} & i_{sq} \end{bmatrix}^T \end{cases}, \tag{2}$$

$$A(t) = \begin{bmatrix} -\gamma & 0 & \frac{K_s}{\tau_r} & K_s n_p \omega(t) \\ 0 & -\gamma & -K_s n_p \omega(t) & \frac{K_s}{\tau_r} \\ \frac{M}{\tau_r} & 0 & -\frac{1}{\tau_r} & -n_p \omega(t) \\ 0 & \frac{M}{\tau_r} & n_p \omega(t) & -\frac{1}{\tau_r} \end{bmatrix}, \tag{3}$$

$$B = \begin{bmatrix} \frac{1}{\sigma L_s} & 0 & 0 & 0 \\ 0 & \frac{1}{\sigma L_s} & 0 & 0 \end{bmatrix}^T, \tag{4}$$

$$C = \begin{bmatrix} 1 & 0 & 0 & 0 \\ 0 & 1 & 0 & 0 \end{bmatrix}, \tag{5}$$

$$v(t) = \begin{bmatrix} v_{sd} & v_{sq} \end{bmatrix}^T, \tag{6}$$

and $\gamma = \frac{1}{\sigma\tau_s} + \frac{1-\sigma}{\sigma\tau_r}, \sigma = 1 - \frac{M^2}{L_s L_r}, K_s = \frac{M}{\sigma L_s L_r}, \tau_S = \frac{L_s}{R_s}, \tau_r = \frac{L_r}{R_r}$.

3. TS fuzzy model of induction machine

The IM model of Eq. (1) could be considered as a linear model whenever the rotor speed is constant. However, when we deal with variable speed application, the model becomes nonlinear and belongs to the well-known class of linear parametric varying models. For application to a wide range of speed, and from an engineering point of view, this term could not be seen as a perturbation in the matrix $A(t)$. Thus, the robust control techniques could not be useful in such an IM application [24]. Hence, other approaches should be adopted to solve this problem. To this end, we propose in this work to use the TS fuzzy method based on the nonlinear sector.

Based on Eq. (1), we consider $z(t) = \omega(t)$ as a nonlinearity term of the matrix $A(t)$.

While considering that $z(t) \in \begin{bmatrix} z_{min} & z_{max} \end{bmatrix}$, the nonlinear term could be presented as follows:

$$z(t) = F_1(z(t))\, z_{max} + F_2(z(t))\, z_{min}, \tag{7}$$

where:

$$\begin{cases} F_1(z(t)) = \frac{z(t) - z_{min}}{z_{max} - z_{min}} \\ F_2(z(t)) = \frac{z_{max} - z(t)}{z_{max} - z_{min}} \end{cases}. \tag{8}$$

Using the TS approach [14,15], the IM nonlinear model of Eq. (1) could be described by fuzzy if-then rules of the following form:

$$\begin{aligned} &\text{if } z(t) is F_i \\ &\text{then } \dot{x}(t) = A_i x(t) + Bu(t), i = \quad 1 \quad \ldots \quad 2 \end{aligned}. \tag{9}$$

The global fuzzy model is inferred as follows:

$$\dot{x}(t) = \sum_{1}^{2} h_i(z(t)) \left(A_i x(t) + Bu(t)\right), \tag{10}$$

$$h_i(z(t)) = \frac{F_i(z(t))}{\sum F_i(z(t))}. \tag{11}$$

For all t, $h_i(z(t)) > 0$ and $\sum_{i=1}^{2} h_i(z(t)) = 1$.

In this section, we have developed a TS IM model described by means of only 2 local models. The purpose is to reduce the conservativeness of the future results compared to other situations where the TS IM model is a blending of 8 linear local models [21–23]. However, it seems that we could not refer to any classical problem in the literature. Indeed, the rotor speed figures simultaneously as a parameter and as an immeasurable decision variable. Thus, the problem could not be treated as an immeasurable state estimation issue [23,25,26]. This challenge was addressed in this work and forms part of the following sections.

4. Synthesis of TS adaptive states observer

To ensure the simultaneous estimation of IM states and rotor speed $\hat{\omega}(t)$, we propose the following adaptive fuzzy full observer:

$$\dot{\hat{x}}(t) = \sum_{i=1}^{2} h_i(\hat{z}(t)) \left(A_i \hat{x}(t) + Bu(t) + L_i \left(y(t) - \hat{y}(t)\right)\right) \ , \tag{12}$$

such that:

$$\hat{z}(t) = \hat{\omega}(t) \ , \tag{13}$$

and

$$\hat{z}(t) = F_1\left(\hat{z}(t)\right) z_{max} + F_2\left(\hat{z}(t)\right) z_{min}, \tag{14}$$

and

$$\begin{cases} F_1\left(\hat{z}(t)\right) = \frac{\hat{z}(t) - z_{min}}{z_{max} - z_{min}} \\ F_2\left(\hat{z}(t)\right) = \frac{z_{max} - \hat{z}(t)}{z_{max} - z_{min}} \end{cases} \ , \tag{15}$$

where $\hat{x}(t)$ denotes the estimated state vector, $\hat{y}(t)$ is the observer outputs, and L_i is the observer gain of the ith local model.

Before presenting the main contribution of this paper, let us state the following definitions and lemmas that we will use in the rest of the paper.

Definition 1 *[27]: A subset D of the complex plane is an LMI region if there exist a symmetric matrix* $\alpha \in \Re^{m*m}$ *and a matrix* $\beta \in \Re^{m*m}$ *such that:*

$$D = \left\{ z \in \mathrm{C} : f_D(z) = \alpha + \beta z + \beta^T \bar{z} \right\}.$$

Lemma 1 *[27]: The matrix A is D-stable if and only if there exists a symmetric positive definite matrix $X>0$ such that:*

$$M_D(A,X) = \alpha \otimes X + \beta \otimes AX + \beta^T \otimes XA^T < 0,$$

where $\otimes$ is the Kronecker product.

Lemma 2 *[28]: Let $D^\sharp = \bigcap_{i=1}^{r} D_i$ such that D_i is a subset such that:*

$$M_{D_i}(A,X) = \alpha_i \otimes X + \beta_i \otimes AX + \beta_i^T \otimes XA^T < 0.$$

The matrix A is $D^\sharp$-stable if and only if there exists a symmetric positive definite matrix $X>0$ such that:

$$\begin{array}{l} M_{D^\sharp}(A,X) = \alpha_i \otimes X + \beta_i \otimes AX + \beta_i^T \otimes XA^T < 0 \\ i = 1 \ldots\ldots r \end{array}.$$

In the following work, we will focus on the $D^\sharp$-stability analysis described by the intersection between vertical stripe D_1, characterized by (α_1, β_1) such that $a_2 < reel(z) < a_1$, and a horizontal stripe D_2, described by (α_2, β_2) such that $|Im(z)| < b$. We use the concept of LMI regions for formulating investment objectives into LMI terms.

Proposition 1 *The adaptive flux fuzzy observer of Eq. (12) is stable with a guaranteed $D^\sharp$-stability analysis if there exist matrices $X>0$ and W_i such that the following LMIs are satisfied:*

$$\left\{ \begin{array}{l} X > 0 \\ \left[\begin{array}{cc} \Theta_i & 0 \\ 0 & \Lambda_i \end{array} \right] < 0 \\ \left[\begin{array}{cc} -2bX & \Xi_i \\ -\Xi_i & -2bX \end{array} \right] < 0 \\ i = 1 \ldots\ldots n \end{array} \right. , \tag{16}$$

where:

$$\left\{ \begin{array}{l} \Theta_i = XA_i - W_iC + A_i^T X - C^T W_i^T - 2a_1 X \\ \Lambda_i = -XA_i + W_iC - A_i^T X + C^T W_i^T + 2a_2 X \\ \Xi_i = XA_i - W_iC - A_i^T X + C^T W_i^T \end{array} \right. .$$

The observer matrix gain will be determined such that:

$$L_i = W_i^T X^{-1}, \tag{17}$$

and the estimated rotor speed $\hat{\omega}(t)$ is identified by the following adaptive scheme:

$$\begin{array}{rcl} \hat{\omega}(t) & = & \frac{1}{\lambda} \sum_{i=1}^{2} g_i(z(t))(\hat{x}(t)^T A_i^T X e_n + e_n(t)^T X A_i \hat{x}(t) \\ & & + e(t)^T C^T L_i^T A_i^T X e_n + e_n(t)^T X L_i C e(t)) \end{array} , \tag{18}$$

where $g_i(z(t))$ *is synthesized as follows:*

$$\begin{cases} g_1\left(z(t)\right) = \frac{2}{z_{max}-z_{min}} \\ g_2\left(z(t)\right) = \frac{-2}{z_{max}-z_{min}} \end{cases} . \tag{19}$$

$e_n(t)$ *is defined as follows:*

$$e_n(t)^T = \left[\begin{array}{cccc} \left(i_{sd} - \hat{i}_{sd}\right) & \left(i_{sq} - \hat{i}_{sq}\right) & 0 & 0 \end{array} \right],$$

and λ *is an arbitrary positive gain.*

Proof We define the error vector as follows:

$$e(t) = x(t) - \hat{x}(t). \tag{20}$$

By differencing Eq. (20), we obtain the error dynamics:

$$\dot{e}(t) = \sum_{i=1}^{2} h_i(z(t)) \left(\left(A_i - L_i C\right) e(t) \right) + \left(\sum_{i=1}^{2} h_i(z(t)) - \sum_{i=1}^{2} h_i(\hat{z}(t)) \right) \left(A_i \hat{x}(t) + L_i C e(t) \right). \tag{21}$$

Considering the Lyapunov function V candidate such that:

$$V = e(t)^T X e(t) + \frac{\lambda}{2} \Delta\omega(t)^2, \tag{22}$$

where $\Delta\omega(t) = \omega(t) - \hat{\omega}(t), X > 0$, and λ is a positive constant.

The derivate of the Lyapunov function in Eq. (22) could be synthesized such that:

$$\dot{V} = \dot{V}_1 + \dot{V}_2 \ , \tag{23}$$

while $\dot{V}_1$ and $\dot{V}_2$ are defined as follows:

$$\dot{V}_1 = \sum_{i=1}^{2} h_i(\hat{z}(t)) \left[e(t)^T \left(A_i - L_i C\right)^T X e(t) + e(t)^T X \left(A_i - L_i C\right) e(t) \right], \tag{24}$$

$$\begin{array}{l} \dot{V}_2 = \left(\sum_{i=1}^{2} h_i(z(t)) - \sum_{i=1}^{2} h_i(\hat{z}(t)) \left[e(t)^T C^T L_i^T A_i^T X e(t) + e(t)^T X L_i C e(t) + \right. \right. \\ \left. \left. \hat{x}(t)^T A_i^T X e(t) + e(t)^T X A_i \hat{x}(t) \right] + \lambda \Delta\omega(t) \Delta\dot{\omega}(t) \right. \end{array} . \tag{25}$$

In the first step, we will consider $\dot{V}_1 < 0$. In addition, we will focus at the same time on the problem of the $D^\sharp$-stability of the matrix $\sum_{i=1}^{2} h_i(z(t)) \left(A_i - L_i C\right)$ via the assignment of the value of the imaginary component of the poles, as well as the response time of the observer via the assignment of the real part of the pole if there exists a matrix $X > 0$ and W_i such that the following inequalities are satisfied:

$$\begin{array}{l} \alpha_j \otimes X + \beta_j \otimes \sum_{i=1}^{2} h_i(z(t)) \left(A_i - L_i C\right) X + \beta_j^T \otimes X \sum_{i=1}^{2} h_i(z(t)) \left(A_i - L_i C\right)^T < 0 \\ j = 1 \ldots\ldots r \end{array} . \tag{26}$$

While considering $L_i = W_i^T X^{-1}$, the bilinear inequality system of Eq. (26) is equivalent to the LMIs described in Eq. (16) [29]. □

In the second step, we will consider $\dot{V}_2 = 0$.

While considering Eq. (19), the subderivative Lyapunov $\dot{V}_2$ function could be presented such that:

$$\dot{V}_2 = \Delta\omega(t)(\sum_{i=1}^{2} g_i(z(t)) - \sum_{i=1}^{2} g_i(\hat{z}(t)))\left[e(t)^T C^T L_i^T A_i^T X e(t) + e(t)^T X L_i C e(t) + \hat{x}(t)^T A_i^T X e(t) + e(t)^T X A_i \hat{x}(t)\right] + \lambda \Delta\omega(t)\Delta\dot{\omega}(t) \quad . \tag{27}$$

Under an assumption such that $\hat{\Psi}_r \to \Psi_r$, we define $e_n(t)$ as follows:

$$e_n(t)^T = \left[\begin{array}{cccc} \left(i_{sd} - \hat{i}_{sd}\right) & \left(i_{sq} - \hat{i}_{sq}\right) & 0 & 0 \end{array}\right].$$

The estimated rotor speed $\hat{\omega}(t)$ is then identified by the following adaptive scheme:

$$\hat{\omega}(t) = \frac{1}{\lambda} \sum_{i=1}^{2} g_i(z(t)) \left(\hat{x}(t)^T A_i^T X e_n + e_n(t)^T X A_i \hat{x}(t) + e(t)^T C^T L_i^T A_i^T X e_n + e_n(t)^T X L_i C e(t)\right) .$$

5. Simulation and experimental results

In this section, simulation and experimental results are presented to evaluate the effectiveness of the proposed control scheme for an IM.

Figure 1 shows the block diagram of the proposed sensorless Indirect field oriented control IRFOC of the IM drive system. The block diagram consists of an IM, a PWM voltage source inverter, an IRFOC block control, a coordinate translator, and a fuzzy adaptive flux observer.

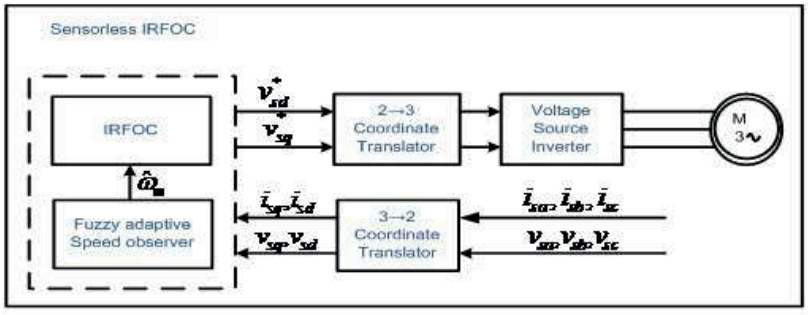

Figure 1. Block diagram of sensorless IRFOC of induction motor drive system.

We will refer to the IRFOC scheme developed in [30] (Figure 2).

In the following, we will consider that the IM operates in a range of 400 rps in the forward and reverse directions, such that the minimal and maximal values of the nonlinearity are $\omega(t) \in [-400rps \;\; 400rps]\,/rps \to$ (radian per second). A check of the observability property is guaranteed, thanks to the observability of local IM TS models.

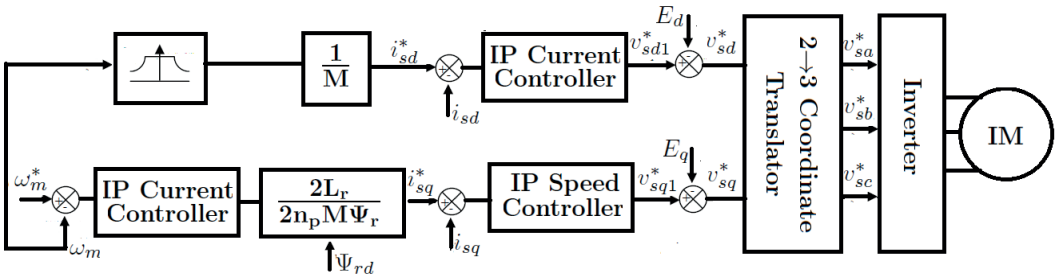

Figure 2. IRFOC structure.

A look at local poles of the IM (Figure 3) shows that they are limited by a real value of –134 and an imaginary value of 800. Therefore, poles of the TS adaptive observer should satisfy some circumstances. Indeed, the real values have to be necessarily at least 2 times faster than these of the IM. In addition, the observer must have an oscillating dynamic very similar to that of the IM. Moreover, since dSPACE has a maximum value of sampling time, the observer dynamic should be slower than the maximum dynamic that could be computed by dSPACE. A deep search was carried out to choose the best LMI region adequate to the pole assignment of the dynamic of the observation error (disk, conic sector, half plane, vertical band, horizontal band). On the basis of this study, we chose to use a clustering of a vertical and a horizontal band, which makes the best compromise between pole assignment objectives and results conservativeness.

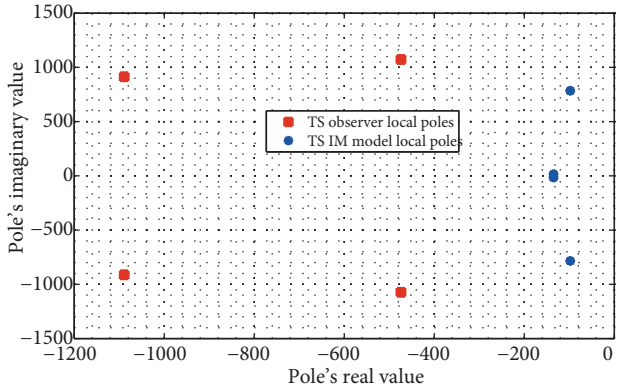

Figure 3. Local poles' position for both TS observer and induction machine TS model.

While considering Proposition 1 and solving the LMIs of Eq. (16) such that $a_1 = -3000, a_2 = 0$, and $b = 1500$, Figure 3 illustrates the position of local poles of the TS IM model and that of the TS adaptive observer. We remark that the $D^\sharp$-stability of the observer is well guaranteed. Indeed, it is at least 2 times faster than the machine, with a limited oscillation dynamic, and there is a guarantee of a minimum of a real pole value to ensure the implementation of the observer algorithm in dSPACE 1104. We note that the choice of $a_2 = 0$ was made to decrease conservativeness while resolving the LMI inequalities. However, at the same time, we verified the local observer poles' placement relative to the IM ones. Future work will have to consider the possibility of presenting a less conservative condition to automatically resolve this problem.

The gain matrices L_i and the matrix X are obtained as follows:

$$L_1 = 10^3 \begin{bmatrix} 1.3302 & -0.6403 \\ 0.6403 & 1.3302 \\ -0.0234 & -0.0545 \\ 0.0545 & -0.0234 \end{bmatrix} L_2 = 10^3 \begin{bmatrix} 1.3302 & 0.6403 \\ -0.6403 & 1.3302 \\ -0.0234 & 0.0545 \\ -0.0545 & -0.0234 \end{bmatrix},$$

$$X = \begin{bmatrix} 0.0001 & 0 & 0.0003 & 0 \\ * & 0.0001 & 0 & 0.0003 \\ * & * & 0.0150 & 0 \\ * & * & * & 0.0150 \end{bmatrix}.$$

6. Simulation results

To verify the dynamic performances of the proposed algorithm, we present a simulation study using MATLAB/Simulink software. During this test, a trapezoidal rotor speed reference is considered. Indeed, the reference speed moves from an initial value of 0 rps at $t = 0s$ to reach a value of 120 rps at $t = 1s$. It is then changed from $t = 10s$ to reach 20 rps at $t = 11s$. During this test, a 7 Nm load torque value is applied during $t = [3s8s]$ and $t = [13s18s]$.

Figure 4 presents the main results of this test. Figure 4a shows the evolution of the rotor speed reference, the real rotor speed, and the estimated rotor speed. Some zooms are presented in the same figure to describe

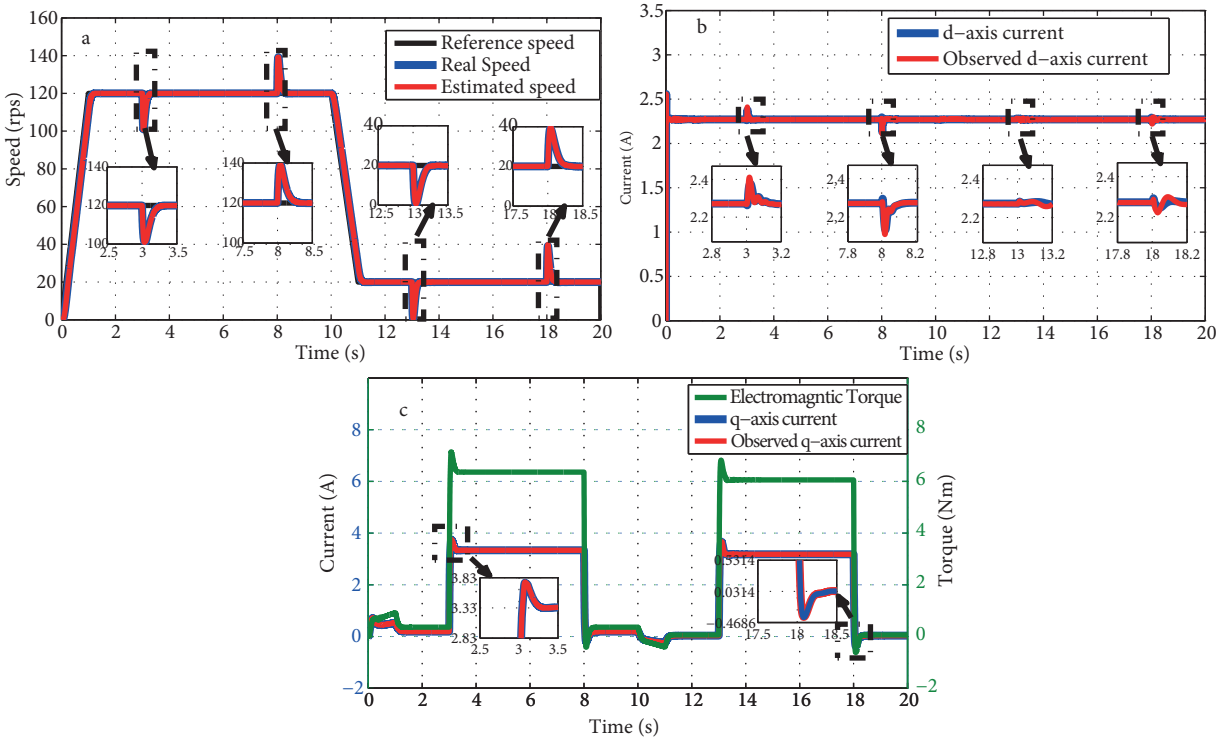

Figure 4. Simulation results.

some transient states characterized by the application and the removal of the load torque. We note that the estimated speed perfectly follows the real one, even during transitory states. In Figures 4b and 4c, we describe the evolution of d-q components of the stator currents in a synchronous rotating reference frame relative to the real ones. In addition, some zooms are presented to best analyze the estimation attitude, especially in transient states. Moreover, in Figure 4c, the electromagnetic load torque waveform is described. We notice that the electromagnetic torque is the same shape as the q components of the stator currents. However, the d component of the stator currents is maintained as constant during all operating modes. Thus, we can conclude that a decoupled control of the flux and torque is obtained.

7. Experimental results

A prototype implementation of the proposed algorithm was carried out (Figure 5). The experimental setup is composed of squirrel cage IM, an insulated gate bipolar transistor (IGBT) source voltage inverter, a real-time DSP1104 controller card, an incremental encoder with 5000 pulses per revolution, 2 voltage sensors, and 3 Hall effect current sensors for the measurement of stator currents. A load torque is generated through the control of a magnetic power brake. The characteristics of the IM 1.5 kW parameters are listed in the Table.

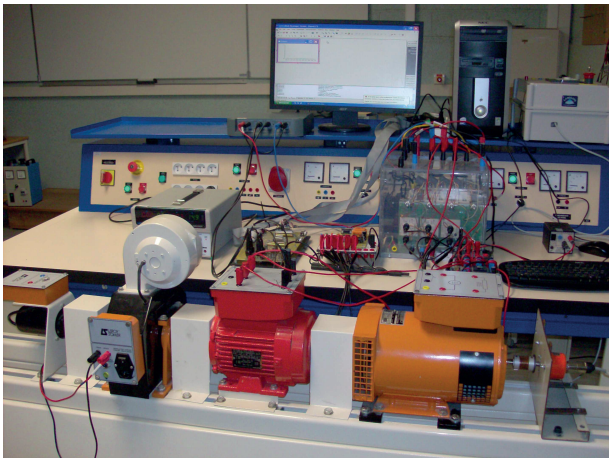

Figure 5. Experimental setup.

Table. Induction machine parameters.

$R_s = 5.72\Omega$	$R_r = 4.2\Omega$
$L_s = 0.462H$	$L_r = 0.462H$
$M = 0.4402H$	$J = 0.0049Kg.m^2$
$f = 0.003N.m.s.rd^{-1}$	$n_p = 2$

For better results verification and evaluation, we present 2 tests in this section, described as follows:

Test 1: In this test, we check the performance of the machine for a high-speed operating mode under different load torque applications. The speed references move from an initial value of 0 rps to attain 120 rps at $t = 2s$, then changes from $t = 9s$ to reach the same value in the reverse direction at $t = 13s$. During this test, a load torque with a value of 4 Nm is applied for a period of $3s$ in $t = 4s$ and $t = 15s$.

Figure 6 includes the first part of the experimental results. Figure 6a shows the evolution of the rotor speed reference, the real rotor speed, and the estimated rotor speed. The speed estimation error is described

in Figure 6b. Figures 6c and 6d show the evolution of d-q (alpha-beta) components of the observed stator currents relative to the real ones (in the stationary reference frame). Figure 7 includes the second part of the experimental results. Thus, we present the d-q components of the observed and the real stator currents, in a synchronous rotating frame, in Figures 7a and 7b. The estimation errors of the stator current components are shown in Figures 7c and 7d.

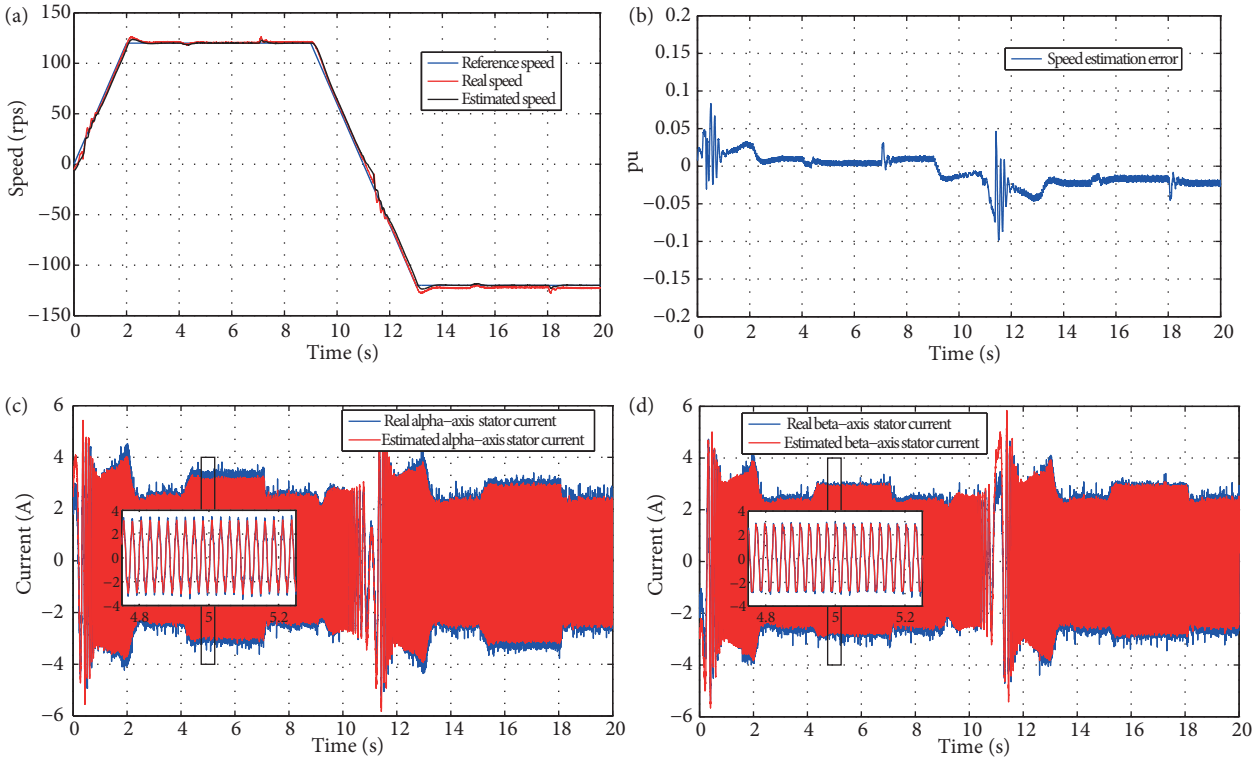

Figure 6. Experimental results of Test 1 (high-speed operation mode).

During this test, the proposed approach provides a perfect speed estimation and tracking despite the disturbance caused by the application load torque. A small gap between the estimated and real values of both the rotor speed or the components of the stator currents is remarkable during acceleration or deceleration phases. However, these error signals are minimized in a steady state.

Test 2: In this test, we check the performance of the machine in low-speed operation mode. The speed references moves from an initial value of 0 rps to 20 rps at $t = 1s$, then changes from $t = 10s$ to reach the same speed in the reverse direction at $t = 11s$. During this experiment, a small value of load torque is applied to test the robustness of the proposed algorithm for a period of $3s$ in $t = 4s$ and $t = 15s$.

Figure 8 presents the first part of the experimental results. First, the evolution of the rotor speed reference, the real rotor speed, and the estimated rotor speed signals are shown in Figure 8a. Second, the speed estimation error is described in Figure 8b. Third, the estimated and the real signals of the alpha components of the stator currents are described in Figure 8c. Finally, the evolution of both the estimated and the real beta components of the stator currents are shown in Figure 8d. Figure 9 includes the second part of the experimental results. Indeed, we present the relative evolution of the estimated d-axis current (respectively q-axis current) relative to the real one in Figure 9a (respectively, in Figure 9b). In addition, the d-q components of the stator current estimation error are given in Figures 9c and 9d.

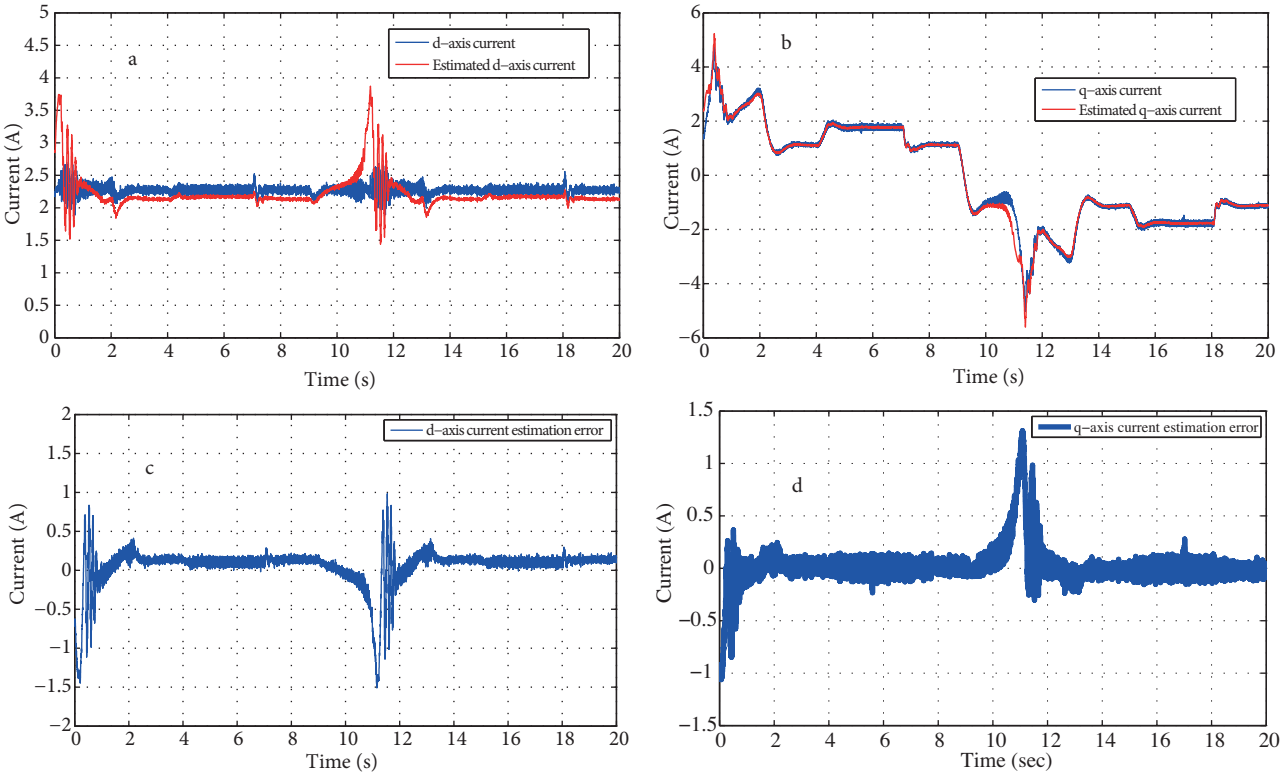

Figure 7. Experimental results of Test 1 (high-speed operation mode).

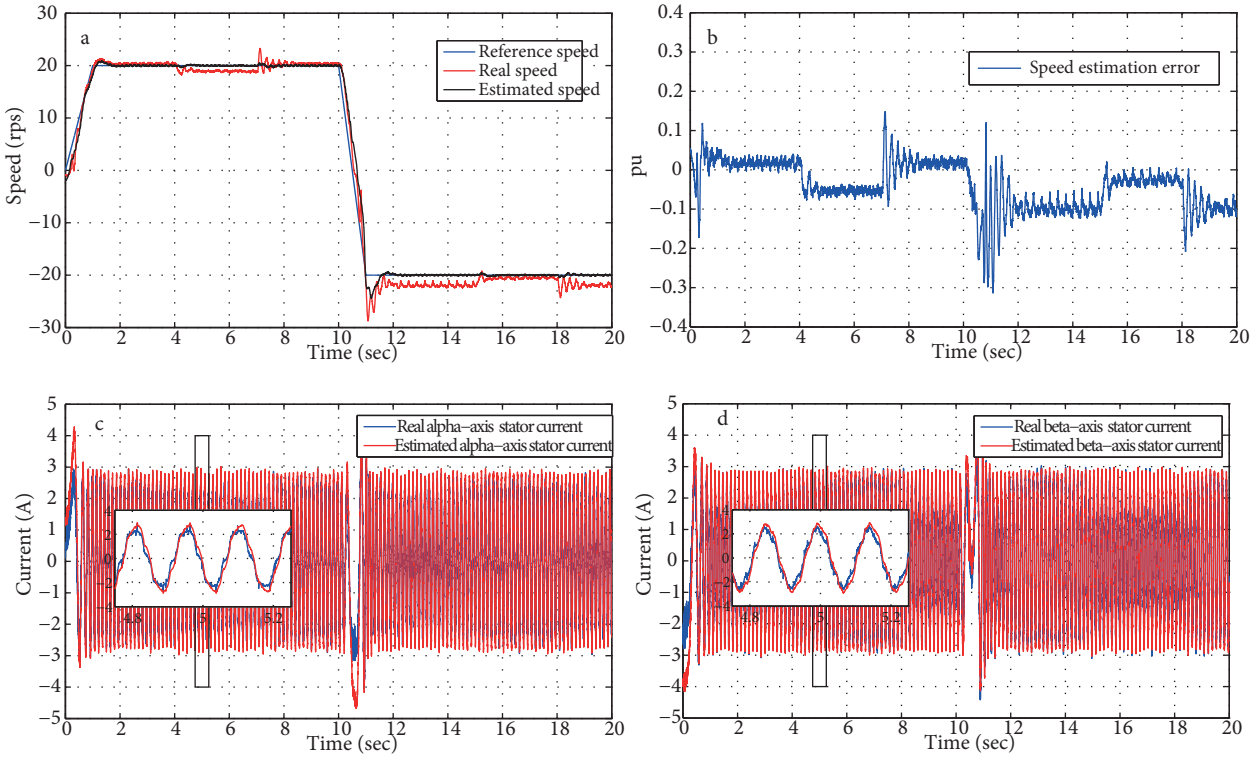

Figure 8. Experimental results of Test 2 (low-speed operation mode).

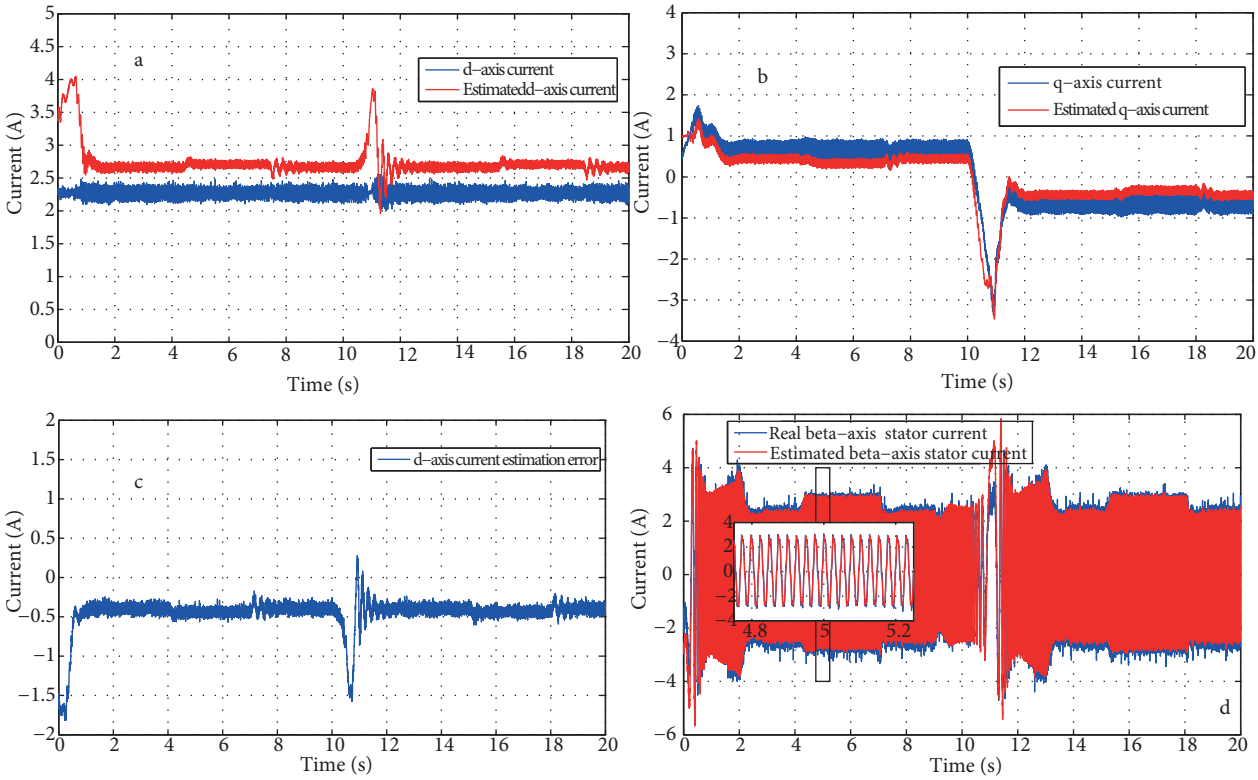

Figure 9. Experimental results of Test 2 (low-speed operation mode).

In this test, the results were less satisfactory; however, they were acceptable. The sensorless speed control and tracking show good performance. Nevertheless, we note an error during current estimation. We can justify this decrease of estimation performance by uncertainties in the IM model and a lack of robustness of the proposed observer.

While comparing the simulation and the experimental results, we note a degradation of the performances of the experimental results relative to the simulations. This degradation can be explained by the fact that, during simulation, neither the dynamic of the inverter nor the imperfection of the machine's parameters and sensors (delay, uncertainties) is considered.

8. Conclusions

In this paper, we have dealt with the sensorless IRFOC control of an IM through the design of a D-stable TS fuzzy adaptive observer based on the Park model in the stationary reference frame. On the basis of an optimal IM TS model design, an adaptive TS fuzzy observer was presented, through which we consider the rotor speed as an immeasurable premise variable. A D-stability study was then given to guarantee a local poles assignment, and a fuzzy speed estimation scheme for the IM was developed. The design conditions were driven in strict LMI terms and still valid for all operating modes. The proposed approach showed perfect performance during simulation testing. In addition, experiments were conducted and confirmed the validity of the proposed results in a real environment and especially for a high-speed operating mode.

Nomenclature

i_{sd}&i_{sq}	Stator currents.
Ψ_{rd}&Ψ_{rq}	Rotor flux.
v_{sd}&v_{sq}	Stator voltages.
v_{sd}&v_{sq}	Stator and rotor resistances.
L_s&L_r	Stator and rotor inductances.
M	Mutual inductance.
σ	Leakage coefficient.
$\omega(t)$	Motor angular velocity.
$\omega_s(t)$	Synchronous angular velocity.
f	Friction constant.
J	Moment of inertia.
n_p	Number of pole pairs.

References

[1] Dominic DA, Chelliah TR. Analysis of field-oriented controlled induction motor drives under sensor faults and an overview of sensorless schemes. ISA T 2014; 53: 1680-1694.

[2] Agrebi Y, Boussak M, Koubaa Y. On line rotor resistance estimation using the model reference adaptive system of induction motor. I-manager's Journal on Electrical Engineering 2010; 3: 1-10.

[3] Alonge F, D'Ippolito F, Sferlazza A. Sensorless control of induction-motor drive based on robust Kalman filter and adaptive speed estimation. IEEE T Ind Electron 2014; 61: 1444-1453.

[4] Menaa M, Touhami O, Ibtiouen R, Fadel M. Sensorless direct vector control of an induction motor. Control Eng Prac 2008; 16: 67-77.

[5] Ur Rehman H, Dhaouadi R. A fuzzy learning sliding mode controller for direct field oriented induction machines. Neurocomputing 2008; 71: 2693-2701.

[6] Lascu C, Boldea I, Blaabjerg F. A class of speed-sensorless sliding-mode observers for high-performance induction motor drives. IEEE T Ind Electron 2009; 56: 3394-3403.

[7] Gadoue S, Giaouris D, Finch J. MRAS sensorless vector control of an induction motor using new sliding-mode and fuzzy-logic adaptation mechanisms. IEEE T Energy Convers 2010; 25: 394-402.

[8] Jouili M, Jarray K, Koubaa Y, Boussak M. Luenberger state observer for speed sensorless ISFOC induction motor drives. Electr Power Syst Res 2012; 89: 139-147.

[9] Korlinchak C, Comanescu M. Sensorless field orientation of an induction motor drive using a time-varying observer. IET Electr Power Appl 2012; 6: 353-361.

[10] Vicente I, Endemano A, Garin X, Brown M. Comparative study of stabilising methods for adaptive speed sensorless full-order observers with stator resistance estimation. IET Control Theory A 2010; 4: 993-1004.

[11] Lokriti A, Salhi I, Doubabi S, Zidani Y. Induction motor speed drive improvement using fuzzy IP-self-tuning controller: a real time implementation. ISA T 2013; 52: 406-417.

[12] Rafa S, Larabi A, Barazane L, Manceur M, Essounbouli N, Hamzaoui A. Implementation of a new fuzzy vector control of induction motor. ISA T 2014; 53: 744-754.

[13] Nounou HN, Ur Rehman H. Application of adaptive fuzzy control to ac machines. Applied Soft Comput 2007; 3: 899-907.

[14] Takagi T, Sugeno M. Fuzzy identification of systems and its applications to modeling and control. IEEE T Syst Man Cy B 1985; 15: 116-132.

[15] Tanaka K, Ikeda T, Wang H. Fuzzy regulators and fuzzy observers: relaxed stability conditions and LMI-based designs. IEEE T Fuzzy Syst 1998; 6: 250-265.

[16] Narimani M, Lam H, Dilmaghani R, Wolfe C. LMI-based stability analysis of fuzzy model-based control systems using approximated polynomial membership functions. IEEE T Syst Man Cy B 2011; 41: 713-724.

[17] Hong SK, Nam Y. Stable fuzzy control system design with pole placement constraint: an LMI approach. Comput Ind 2003; 51: 1-11.

[18] Abbadi A, Nezli L, Boukhetala D. A nonlinear voltage controller based on interval type 2 fuzzy logic control system for multimachine power systems. Int J Elec Power 2013; 45: 456-467.

[19] Tanaka K, Ikeda T, Wang H. Robust stabilization of a class of uncertain nonlinear systems via fuzzy control: quadratic stabilizability, H infinity, control theory, and linear matrix inequalities. IEEE T Fuzzy Syst 1996; 4: 1-13.

[20] Wang H, Tanaka K, Griffin M. An approach to fuzzy control of nonlinear systems: stability and design issues. IEEE T Fuzzy Syst 1996; 4: 14-23.

[21] Allouche M, Chaabane M, Souissi M, Mehdi D, Tadeo F. State feedback tracking control for indirect field-oriented induction motor using fuzzy approach. International Journal of Automation and Computing 2013; 10: 99-110.

[22] Liu P, Hung CY, Chiu CS, Lian KY. Sensorless linear induction motor speed tracking using fuzzy observers. IET Electr Power Appl. 2011; 5: 325-334.

[23] Hung CY, Liu P, Lian KY. Fuzzy virtual reference model sensorless tracking control for linear induction motors. IEEE T Syst Man Cy B 2013; 43: 970-981.

[24] Kchaou M, El Hajjaji A, Toumi A. Non-fragile H-infinity output feedback control design for continuous-time fuzzy systems. ISA T 2015; 54: 3-14.

[25] Moodi H, Farrokhi M. On observer-based controller design for Sugeno systems with unmeasurable premise variables. ISA T 2014; 53: 305-316.

[26] Ichalal D, Marx B, Ragot J, Maquin D. State estimation of Takagi–Sugeno systems with unmeasurable premise variables. IET Control Theory A 2010; 4: 897-908.

[27] Chilali M, Gahinet P. H-infinity design with pole placement constraints: an LMI approach. IEEE T Autom Contr 1996; 41: 358-367.

[28] Chilali M, Gahinet P, Apkarian P. Robust pole placement in LMI regions. IEEE T Autom Contr 1999; 44: 2257-2270.

[29] Boyd S, El-Ghaoui L, Feron E, Balakrishnan V. Linear Matrix Inequalities in System and Control Theory. Philadelphia, PA, USA: SIAM, 1994.

[30] Bahloul M, Souissi M, Chaabane M, Chrifi Alaoui L. Takagi Sugeno fuzzy observer based direct rotor field oriented control of induction machine. In: 2013 Third International Conference on Systems and Control; 29–31 October 2013; Algiers, Algeria. Piscataway, NJ, USA: IEEE. pp. 419-426.